Post-print of: Jarzębowicz L.: "Quasi-discrete modelling of PMSM phase currents in drives with low switching-to-fundamental frequency ratio," in *IET Power Electronics*, vol. 12, no. 12 (2019), pp. 3280-3285 DOI: 10.1049/iet-pel.2018.6285

Quasi-discrete modelling of PMSM phase currents in drives with low switching-to-fundamental frequency ratio

Leszek Jarzebowicz

Faculty of Electrical and Control Engineering, Gdańsk University of Technology, Narutowicza St. 11/12, Gdańsk, Poland
*leszek.jarzebowicz@pg.edu.pl

Abstract: This paper proposes a new quasi-discrete approach to modelling the permanent magnet synchronous motor (PMSM). The quasi-discrete modelling reflects the impact of continuous rotor movement, which takes place during a control cycle, on the shape of motor current waveforms. This provides much improvement in current modelling accuracy under inverter low switching-to-fundamental frequency operation. The proposed approach may be used in predictive control to compute current at forthcoming instants or in classical control to improve precision of determining mean current feedback. The superior accuracy of the quasi-discrete model is confirmed by simulation and experiment for an exemplary PMSM drive operating at inverter switching frequency of 5 kHz and fundamental frequency reaching 400 Hz.

1. Introduction

Permanent Magnet Synchronous Motors (PMSMs) are widely used and appreciated in numerous applications. Contemporarily, there is an increased interest in extending the speed range of electric motors, as this provides savings in drive's weight, volume and losses [1][2]. One of the application fields, where the speed-range extension is clearly notable, is the drivetrain of electric and hybrid cars [3][4]. Nowadays, such cars are typically fitted with electric motors whose speed exceed 10000 rpm. High operating speeds are also desired, for instance, in turbochargers for combustion engines, where rotational speeds reach 80000 rpm [5]

The rotor speed is associated with the fundamental frequency of stator voltage, so high-speed operation requires from the inverter to produce voltage with frequencies at a level of few hundreds hertz. As the switching frequency of the inverter is limited due to the dynamic properties of the transistors, the increase in operating speed results in the reduced ratio between the switching frequency and the fundamental frequency of inverter output voltage (shortly: switching-to-fundamental frequency ratio, SFFR) [6]. Besides high-speed drives, such operating conditions apply to high-power drives, where rotor speeds are moderate, but the switching frequency usually does not exceed a few hundred hertz, so that the SFFR can drop below 10 [7]. Regardless the rated power, low SFFR with a constant value of 6 is used in six-step controlled drives, which provide increased torque at high motor speeds [8].

Although the control principles for drives operating with low SFFR are generally the same as for regular drives, some recent papers indicate problems related to substantial change in the rotor position during a discrete control cycle. Authors of [9] focus on a double transformation of reference frames that is applied in the field oriented control (FOC). First, the measured phase currents are transformed into the field-oriented reference frame in order to deliver feedback for the current controllers. Next, the controllers' output is transformed back to the phase coordinates to set the pulse width modulation (PWM) generator. However, the rotor may cover a significant angular distance between current sampling and inverter output voltage update. Thus, authors of [9] proposed that the inverse reference frame transformation should be carried out using a modified rotor angle, whose value corresponds to the mid-point of the next control cycle. Another paper [10] investigates how digital processing of current feedback affects the accuracy of deriving the mean field-oriented currents. The tackled problem origins from the improper order of operations, where the mean phase currents are derived first and the reference frame transformation is carried out later. In low SFFR drives, this may introduce notable errors in deriving feedback of mean field-oriented currents. Furthermore, a number of papers aim at the problem of voltage distortions in low SFFR drives, e.g. [7][11]. If the SFFR becomes small and when it is not an integer, the output voltage becomes distorted and motor voltages and currents consist of notable subharmonics. To avoid this, various synchronized PWM methods were introduced in order to maintain a round ratio between the switching and the fundamental frequency.

In the last years, predictive control of PMSM has become popular as it provides good control properties with reduced inverter switching frequency [12]. Predictive algorithms are used to compute the future values of motor model state variables based on assumed supplying voltage.

This allows for selecting the optimal sequence of voltages with respect to some predefined criterion. In finite control set (FCS) methods, the voltage is selected from a narrow set corresponding to the fundamental states of the inverter [13]. There are also continuous control set (CCS) algorithms, where the output voltage is provided using modulation techniques. Most predictive control algorithms rely on a mathematical model of the motor (Model Predictive Control, MPC) [14]. The prediction horizon can be a single or multiple control cycles; however, the computational effort rises exponentially with the horizon length. Thus, decreasing the computational demand is one of the main issues of predictive control [15]. Accuracy of the prediction depends on drive's modelling precision. Hence, various on-line parameters identification methods are proposed to increase the robustness to motor model parameters uncertainty [16]. Furthermore, motor model discretization, which is necessary for the microprocessor-based control, has been identified as a source of errors, as reported in [17]. The referenced study proves that discretizing the PMSM model using Euler's approximation, which assumes linear changes of motor current between the discretization steps, results in substantial errors of current prediction. These errors, derived for an exemplary high-speed PMSM drive with the minimal SFFR of 14, approach 40% of the rated current.

A modelling approach that uses the linear current approximation is also commonly applied to the classical closed-loop current control. Due to the use of pulse width modulation, the waveforms of motor voltage and current have a complex shape related to the timing of inverter switching [18]. The high-frequency components in waveforms are beyond the control bandwidth, so the current control operates based on mean voltages and currents. Consequently, the mean value from the rippled motor current must be extracted as the feedback for the current controller. This problem is usually solved by sampling the motor phase currents synchronously with the peaks of symmetrical PWM carrier, i.e. sampling at the mid-points of PWM cycles [19]. Using the continuous-time motor model supplemented by the assumption of linear current changes upon steady voltage intervals, the mid-point sample corresponds to the mean current in a PWM cycle. However, the assumption of linear current changes has been recently reported erroneous under specific conditions, such as short electrical time constant of the motor or low SFFR operation. The first case was analysed by Wolf at al. [20]. The authors reported substantial errors of mean current measurement by the synchronous sampling in case of low stator inductance-to-resistance ratio. In turn, another paper [21] focuses on current modelling errors related to low SFFR operation, where the rotor covers substantial angular distance during a PWM cycle. The synchronous sampling error of 6% was reported for a PMSM drive operating with SFFR of 14.

The modelling accuracy has an important impact on drive's properties. By improving this accuracy, the motor currents may be controlled more precisely, which leads to less torque ripples, better utilisation of inverter input voltage and improvement in the efficiency. Also, the content of higher harmonics in motor currents may be decreased, so that the total harmonic distortions are minimized. As reviewed above, important limitations of the classical PMSM modelling, which involves the linear current changes assumption, were recognized in the context of low SFFR operation. The referenced papers, related to low SFFR operation, aim at quantifying errors related to the classical modelling. This paper proposes a quasi-discrete approach to modelling PMSM, which constitutes a solution to the problems identified in the previous work. The approach reflects non-linear current changes related to the continuous advancement in rotor position. Although the model consists of a continuous-time term, it still may be used for deriving the mean current or predicting the future current in a microprocessor-implemented algorithm, as explained in further sections. The accuracy of the model was verified by simulation and experiment for a high-speed PMSM drive with the minimal SFFR of 12.5.

2. Standard approach to mean current derivation

The model, which is in the background of the synchronous current sampling technique, relies on a set of assumptions [19][20]. First, the current waveform in a PWM cycle is decomposed into fundamental and ripple components (Fig. 1). The first component is a theoretical response to a constant supplying voltage, whose value is equal to the mean voltage in the PWM cycle. Current derivative is assumed constant in steady-voltage intervals, so the current fundamental component changes linearly throughout the PWM cycle, as in Fig. 1a.

The current ripple component is a response to a voltage, whose value is defined as a difference between instantaneous and mean voltage. If the voltage waveform is symmetrical, the waveform of ripple component crosses zero at the mid-point and at the boundaries of PWM cycle. Moreover, the mean of the ripple component equals zero. These properties cause that the mean current is related solely to the fundamental component waveform, which changes linearly. This provides the opportunity to extract the mean current by using a single sample that is acquired at the mid-point of PWM cycle [19][22].

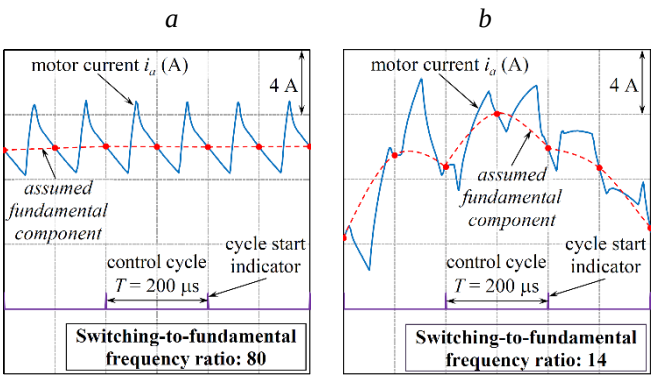

Fig. 1. *PMSM phase current waveforms recorded in a laboratory drive operating with switching frequency of 5 kHz and fundamental inverter output frequency of:* **(a)** 60 Hz, **(b)** 350 Hz

3. Standard approach to discretizing PMSM model for current predictive control

The continuous-time model of non-salient PMSM can be formulated using a vector notation:

$$\frac{d\mathbf{i}(t)}{dt} = \frac{1}{L}\left(-R\mathbf{i}(t) + \mathbf{u}(t) + \mathbf{e}(t)\right) \tag{1}$$

where: $\boldsymbol{i}(t)$, $\boldsymbol{u}(t)$, $\boldsymbol{e}(t)$ are vectors representing motor current, voltage and electromotive force (EMF), respectively; L is stator inductance and R is stator resistance.

In order to solve the model in a digital controller, the continuous-time equation (1) must be discretized. This discretization typically uses the forward Euler approach, which approximates the current derivative with the difference quotient:

$$\frac{d\mathbf{i}^{[k]}}{dt} \cong \frac{\Delta\mathbf{i}^{[k]}}{T} = \frac{\mathbf{i}^{[k+1]} - \mathbf{i}^{[k]}}{T} \tag{2}$$

where the discretization step is equal to the control cycle duration T (inverse of the switching frequency), and the discrete current values $i^{[k]}$, $i^{[k+1]}$ correspond to the start-points of subsequent control cycles.

According to (1) and (2), the current at the beginning of the forthcoming (k+1)-th cycle can be predicted using the model variables determined at the beginning of k-th cycle [13][23][24]:

$$\mathbf{i}^{*[k+1]} = \mathbf{i}^{[k]} + \Delta\mathbf{i}^{*[k]} = \mathbf{i}^{[k]} + \frac{T}{L}\left(-R\mathbf{i}^{[k]} + \mathbf{u}^{[k]} + \mathbf{e}^{[k]}\right) \tag{3}$$

where "*" indicates a predicted value.

Continuous control set (CCS) predictive methods use voltage modulation to obtain an infinite set of control outputs. In such a case, the motor model uses the mean voltage, so only the current fundamental component is reproduced. As the fundamental component is equal to the actual current at start-points and at mid-points of the control cycle, this approach is suitable for predicting instantaneous current values corresponding to the beginnings of forthcoming control cycles.

According to (3), the current change $\Delta i^{*[k]}$ is proportional to the cycle duration T. Consequently, the value of the fundamental current derivative is assumed not to change during the discretization period T.

4. Impact of low SFFR operation on modelling motor current

As indicated in the literature review, the linear current approximation was reported erroneous in short time-constant drives [20] and in low switching-to-frequency ratio drives [21]. This paper focuses on the latter case, with the origin of the modelling problem explained below.

The major impact on the current derivative di/dt in (1) is applied by the imbalance between voltage and EMF vectors, i.e. by the u(t)+e(t) term. If the stationary reference frame is used, the motor voltage vector can be assumed constant during the control cycle, but the EMF vector rotates synchronously with rotor position θ:

$$\mathbf{e}(t) = \left(\omega \cdot \psi_f\right)\exp\left(\mathbf{j}(\theta(t) + \pi/2)\right) \tag{4}$$

where: ω – rotor speed; ψ_f – permanent magnets flux linkage.

Since the angle of the EMF vector is fixed to the rotor, and in low SFFR drives the rotor position $\theta(t)$ may advance by tens of degrees during T, the value of $u(t)$+$e(t)$ can distinctively change in a control cycle. This, in turn, causes that the current derivative varies in time, making the assumption of linear current changes over simplistic.

5. Quasi-discrete modelling of PMSM current

In order to improve the modelling accuracy under low SFFR operating conditions, a quasi-discrete model is proposed. This model reflects the varying value of the current derivative during the control cycle, which is related to the continuous motion of the rotor:

$$\frac{d\mathbf{i}(t)}{dt} \cong \frac{1}{L}\left(-R\mathbf{i}^{[k]} + \mathbf{u}^{[k]} + \mathbf{e}^{[k]} \cdot \exp(\mathbf{j}(\omega^{[k]} \cdot t))\right) \tag{5}$$

where: $t \in \langle 0, T)$ is the duration of k-th control cycle.

The quasi-discrete model withdraws the assumption of constant EMF vector angle in the control cycle. In both models (3) and (5), the **e** vector is computed based on the sampled rotor speed $\omega^{[k]}$ and position $\theta^{[k]}$, so that it corresponds to the start-point of the control cycle. However, in the quasi-discrete model the EMF vector continues to rotate throughout the control cycle. The continuous advancement in the EMF vector angle, caused by the exponential function in (5), is modelled with the assumption of constant rotor speed $\omega^{[k]}$. This assumption is well justified due to relatively large mechanical moment of inertia. Consequently, the quasi-discrete model uses the same discrete variables as (3), but the part associated to the EMF is extended with the additional continuous-time term that reflects the rotor movement within the control cycle. This term makes the model (5) not fully discrete. Nevertheless, both mean determination and current prediction require integrating (5) with respect to time. This integration, which turns the continuous-time term into a constant, can be carried out offline using analytical methods. Hence, the quasi-discrete model is fully applicable to the algorithms that are executed discretely.

The details on the practical applications of the quasi-discrete model are given in the following sections. In order to provide a concise description, the proposed approach is explained on the example of modelling the A-phase current, for which the quasi-discrete model may be re-formulated as follows:

$$\frac{di_A(t)}{dt} \cong \frac{1}{L}\left(-Ri_A^{[k]} + u_A^{[k]} + \psi_f \cdot \omega^{[k]} \cdot \sin\left(\theta^{[k]} + \omega^{[k]} \cdot t\right)\right) \tag{6}$$

In the above equation, the continuous-time term that reflects the advancement of the EMF vector angle by $\omega^{[k]} \cdot t$ is included directly in the argument of sine function, which computes the A-phase component of the electromotive force. Modelling the other phase currents may be approached in a similar manner.

6. Quasi-discrete approach to determining the mean current

The mean A-phase current in the k-th control cycle is defined as:

$$\bar{i}_A^{[k]} = \frac{1}{T}\int_0^T i_A(t)dt \tag{7}$$

The current waveform in (7) is considered as:

$$i_A(t) = i_A(t=0) + \Delta i_A(t) \tag{8}$$

where the start-point value $i_A(t = 0)$ may be derived by sampling the phase current, and the current increase $\Delta i_A(t)$ can be reproduced using the quasi-discrete model (6) as follows:

$$\begin{aligned}\Delta i_A(t) &= \int_0^t \frac{di_A(t)}{dt}dt = \\ &\cong \frac{u_A^{[k]}t - Ri_A^{[k]}t + \psi_f \cdot \cos\left(\theta^{[k]}\right) - \psi_f \cdot \cos\left(\theta^{[k]} + \omega^{[k]} \cdot t\right)}{L}\end{aligned} \tag{9}$$

Consequently, the mean current is derived as:

$$\begin{aligned}\bar{i}_A^{[k]} &= i_A^{[k]} + \frac{1}{T}\int_0^T \Delta i_A(t)dt = \\ &= i_A^{[k]} + \frac{u_A^{[k]}T - Ri_A^{[k]}T}{2L} + \frac{\psi_f \cos\left(\theta^{[k]}\right)T}{L} + \\ &- \frac{\psi_f \cdot \sin\left(\theta^{[k]} + \omega^{[k]} \cdot T\right) - \psi_f \cdot \sin\left(\theta^{[k]}\right)}{L\omega^{[k]}T}\end{aligned} \tag{10}$$

The formula (10) consists solely of the discrete variables, which are available by default in a digital controller. The last term of (10) includes motor speed in denominator. Thus, the practical application should use a floating-point processor in order to assure sufficient accuracy during low speed operation, if the method is expected to cover whole operational speed range.

7. Quasi-discrete approach to current prediction

Predicting the current corresponding to the start-point of (k+1)-th control cycle is carried out similarly to the standard approach (3), i.e. by using the current sample $i_A^{[k]}$ from the start-point of k-th cycle and the current change $\Delta i_A^{[k]}$ computed based on the motor model:

$$i_A^{*[k+1]} = i_A^{[k]} + \Delta i_A^{[k]} \tag{11}$$

The difference lies in the computation of the current change $\Delta i_A^{[k]}$. In the proposed approach, this change is derived using the quasi-discrete model:

$$\begin{aligned}\Delta i_A^{[k]} &= \int_0^T \frac{di_A(t)}{dt}dt = \\ &\cong \frac{u_A^{[k]}T - Ri_A^{[k]}T + \psi_f \cdot \cos\left(\theta^{[k]}\right) - \psi_f \cdot \cos\left(\theta^{[k]} + \omega^{[k]} \cdot T\right)}{L}\end{aligned} \tag{12}$$

Similar to the mean current derivation formula (10), the current prediction formula (12) consists of only discrete variables, which allows for its practical implementation.

8. Verification by simulation

Effectiveness of the proposed approach is first verified by simulation carried out in Simulink. The model was designed to reproduce continuous waveforms of motor currents as well as discrete events related to microprocessor-based control. For the latter, the Simulink's triggered subsystems were applied as described in [25].

The general structure of the simulation model is presented in Fig. 2. The grey blocks in Fig. 2 represent operations, which are executed discretely, once per PWM cycle. Their execution is triggered either by valleys or by peaks of PWM carrier signal (shown in Fig. 3), so it takes place at the start-points or mid-points of the control cycle, respectively. Discrete signals are marked with white arrowheads. In contrast, white blocks correspond to subsystems running continuously and continuous-time signals are marked with black arrowheads.

The PMSM is modelled as a continuous-time subsystem based on (1). The drive uses standard field-oriented current control algorithm, whose feedback consists of motor phase currents sampled synchronously at the mid-points of PWM cycle. The parameters of the model were set up to represent a laboratory drive (Table 2), which is used for experimental validation described in Section 9. The drive operates with constant switching frequency of 5 kHz. The maximum inverter fundamental frequency is 400 Hz, which corresponds to the minimal SFFR of 12.5.

The model of PMSM drive reproduces the phase currents waveforms, from which the A-phase current is further processed in order to evaluate the standard and proposed methods. Separating the evaluation from the control enables for comparing the results of different methods for identical operating conditions.

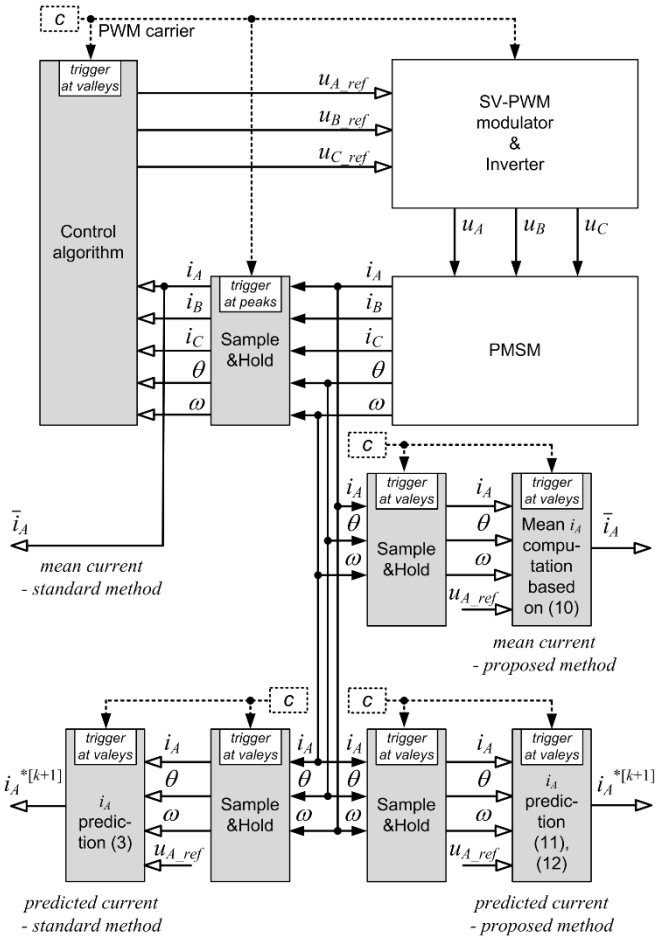

Fig. 2. *General structure of the simulation model*

The mean phase current is derived both by synchronous mid-point sampling and by the proposed formula (10) that originates from the quasi-discrete model. The results of both methods are compared with numerically computed mean of the current waveform (not shown in Fig. 2) in order to derive errors. The reference value of the mean current is available at the end of the PWM cycle. In contrast, the proposed and standard methods update their results at the start-point and at the mid-point of the cycle, respectively. Thus, all the signals are synchronized before computing the errors. The errors of standard and proposed current prediction methods are derived one control cycle after the prediction update, by comparing the predicted current with the sample of actual motor current. The timing schemes of the above-described events are given in Fig. 4 and Fig. 5, separately for mean derivation methods and current prediction methods.

The waveforms of the errors recorded for steady operation at the maximal speed are presented in Fig. 6, along with the sampled phase current waveform. All the error waveforms are quasi-sine shaped, so their maximal value correspond to the waveform amplitudes. The maximal errors of determining the mean current are 0.28 A and 0.04 A for the standard and the proposed method, respectively. This constitutes a 7-times improvement. In case of current prediction methods, the ratio between the errors of proposed and standard methods is even greater and equals 3.30 A/0.12 A = 27.5 Concluding, the proposed quasi-discrete modelling approach provides significant improvement both in mean current derivation and in current prediction.

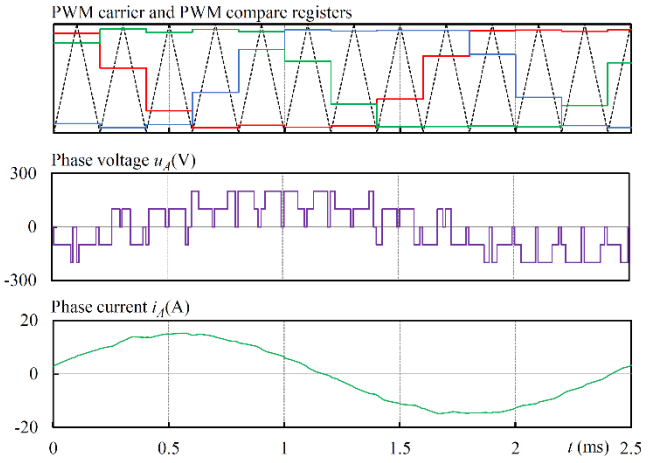

Fig. 3. *Exemplary waveforms of PWM control signals, A-phase voltage and A-phase current (at maximal rotor speed of 8000 rpm, i.e. SFFR of 12.5)*

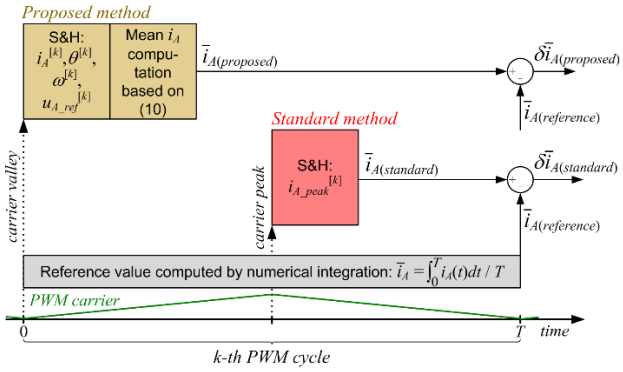

Fig. 4. *Timing of events related to mean current derivation methods*

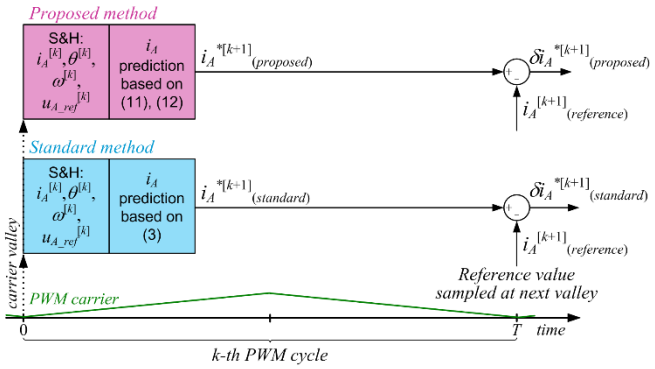

Fig. 5. *Timing of events related to current prediction methods*

The waveforms shown in Fig. 6 correspond to the minimal SFFR in the considered drive. In order to investigate how the errors vary with the SFFR, a set of simulations was carried out for different rotor speeds. In each case, the drive operated with the rated current. The summary of the simulations for SFFR above 50 is presented

in Fig. 7. It uses relative errors, which were computed based on the ratio between the rms of error waveforms and the rms of motor phase current. Error values for selected operating speeds are given in Table 1. In general, the proposed methods deliver more accurate outcomes at any speed. However, at low speeds errors of the standard methods are considered acceptable. For example, the errors derived for running at 500 rpm (SFFR of 200) are lower than the expected errors related to measurement noise and uncertainty of motor parameters. The advantage of using the quasi-discrete modelling becomes evident for the SFFR below 20.

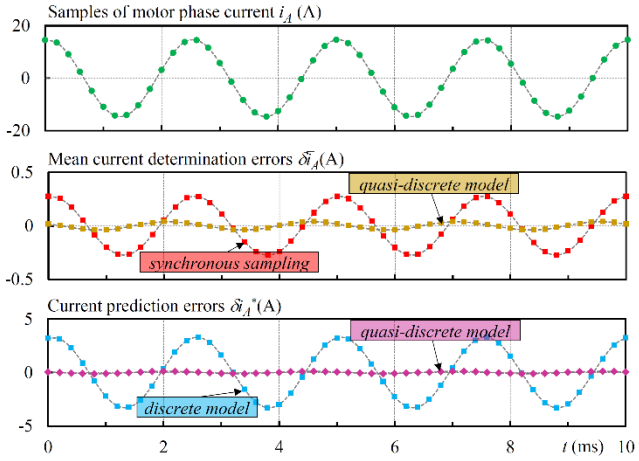

Fig. 6. *Simulation results: waveforms of mean current determination errors and current prediction errors*

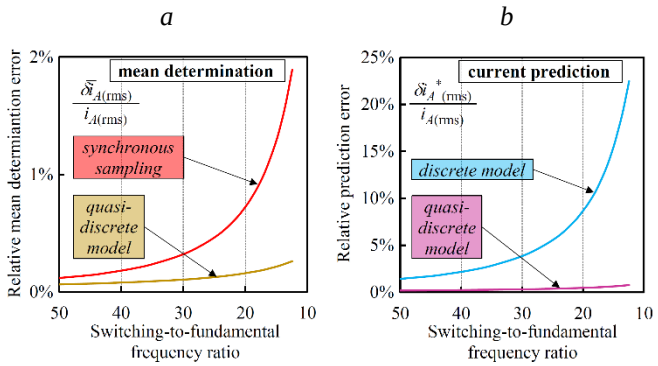

Fig. 7. *Simulation results: waveforms of mean current determination errors* **(a)** *and current prediction errors* **(b)**

Table 1 Selected simulation results

Determined variable	Error for standard method	Error for proposed method
Mean current at 500 rpm (SFFR of 200)	0.041%	0.018%
Predicted current at 500 rpm (SFFR of 200)	0.494%	0.048%
Mean current at 5000 rpm (SFFR of 20)	0.73%	0.16%
Predicted current at 5000 rpm (SFFR of 20)	8.82%	0.47%
Mean current at 8000 rpm (SFFR of 12.5)	1.89%	0.26%
Predicted current at 8000 rpm (SFFR of 12.5)	22.4%	0.76%

9. Verification by experiment

The experimental validation is carried out using a laboratory PMSM drive whose main parameters are given in Table 2. The laboratory setup includes the controller based on a 32-bit fixed-point digital signal processor. The control program uses per-unit variables whose values are stored in IQ24 format. Control program variables are recorded by using a serial link to the host computer.

Table 2 PMSM drive setup

Parameter	Value
Rated power	P_r = 1.5 kW
Inverter's switching frequency	f_{PWM} = 5 kHz
Pole pairs	p = 3
Maximal speed	ω_{max} = 8000 rpm
Rated phase current (rms)	i_r = 10.5 A
Stator inductance	L = 5.2 mH
Stator resistance	R = 0.75 Ω
Permanent magnet flux	ψ_f = 0.134 Wb

The validation is focused on current prediction errors; hence, the errors for the discrete model and the proposed quasi-discrete model are derived similarly to the simulation discussed in the previous section. The timing of events is consistent with Fig. 5.

The waveforms of prediction errors obtained for the maximal speed and the rated current are presented in Fig. 8. In comparison to the simulation results from Fig. 6, the error waveforms are disturbed, which is most likely related to measurement noise and uncertainties of motor parameters. Nevertheless, the shape and amplitude of the error waveform corresponding to the discrete model confirm the most important features derived by simulation. As for the quasi-discrete model, the noise appears to have a major impact on the error. Hence, the modelling inaccuracies that were noted in simulation are not directly observable in the experimental results.

In order to evaluate how the accuracy of current prediction changes with SFFR, a series of recordings was carried out at different rotor speeds. In every case, the PMSM drive operated with rated current. However, the load torque, provided by a DC machine, was adjusted to settle the rotor speed at a value corresponding to the desired SFFR. At steady speed, waveforms of prediction errors for both discrete and quasi-discrete modelling were transferred from the drive controller to the host computer, along with the phase current waveform. The waveforms were post processed to extract rms value from each recorded quantity. Based on rms errors and rms currents, the relative errors were computed. Summary of the post processed results is given in Fig. 9, along with simulation outcomes. Errors values for selected speeds are given also in Table 3. The errors of the discrete model (Fig. 9a) are similar for the simulation and the experiment. In case of the quasi-discrete model (Fig. 9b), the errors obtained in the experiment are substantially higher than in simulation. This leads to a conclusion that the minor modelling inaccuracies of the quasi-discrete model are irrelevant in practical implementation, as their impact on current prediction in much smaller than the impact of measurement noise. Despite this major impact of noise, the experimentally derived errors for the quasi-discrete model at the maximum speed are more than 6 times smaller than that of the discrete model.

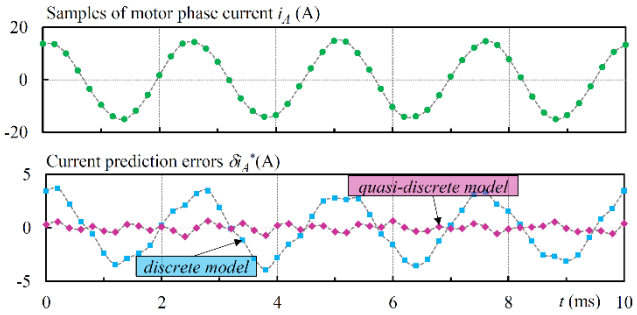

Fig. 8. Experimental results: waveforms of current prediction errors obtained for the maximal speed

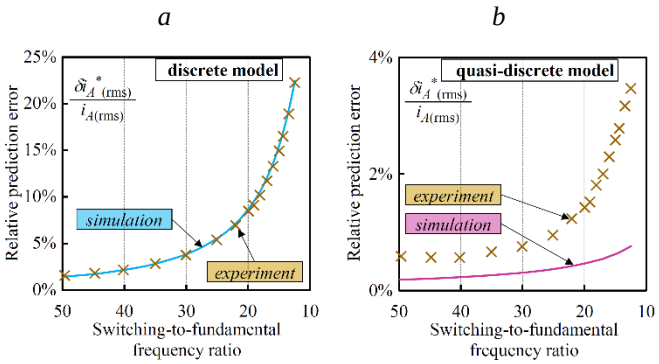

Fig. 9. *Comparison between experimental and simulation results: summary of current prediction errors for discrete modelling* **(a)** *and quasi-discrete modelling* **(b)**

Table 3 Selected experimental results

Determined variable	Error for standard method	Error for proposed method
Predicted current at 5000 rpm (SFFR of 20)	8.96%	1.43%
Predicted current at 8000 rpm (SFFR of 12.5)	22.3%	3.47%

10. Conclusion

The paper proves that the regular modelling of PMSM, which uses linear current approximation, provides insufficient accuracy when the drive operates with low switching-to-fundamental frequency ratio. The proposed quasi-discrete approach significantly improves the modelling accuracy in such a case.

From the two errors that were investigated in the paper, the current prediction error is more dependent on the selection of modelling approach. For the standard discrete modelling and the minimal investigated SFFR, this error exceeded 22%, both in simulation and experiment. In contrast, the quasi-discrete modelling decreased this error into less than 1% in simulation and less than 4% in experiment. It should be commented that the derived errors correspond to a one-cycle prediction horizon, and the application of predictive control commonly use longer horizons. Moreover, the implementation of predictive control requires an additional measurement-delay compensation algorithm that also uses the motor model. Therefore, the prediction errors obtained in the close-loop predictive control are expected to be greater than the ones derived in this paper.

The impact of linear current changes the assumption on the derivation of mean phase current is smaller than on current prediction. The mean current errors derived in simulation for the standard model do not exceed 2% upon SFFR of 12.5. Such a small modelling error would not to be clearly noted in the presence of measurement noise. Nevertheless, applications featured by the SFFR lower than 10 are reported in the references, and the error rises very rapidly with the decrease of SFFR. In such very low SFFR drives the superior accuracy of the proposed quasi-discrete model may be beneficial.

This study focuses on PMSM, but similar modelling problems appear in induction motors, which are more often used in high power drives operating at very limited switching frequencies. In this regard, the proposed discretization approach may be considered as a versatile solution.

11. Acknowledgments

This work was financially supported by the National Science Centre Poland (Grant no. 2018/02/X/ST7/00488).

12. References

[1] Gerada, D., Mebarki, A., Brown, N.L., Gerada, C., Cavagnino, A., Boglietti, A.: 'High-Speed Electrical Machines: Technologies, Trends, and Developments', IEEE Transactions on Industrial Electronics, 2014, 61, (6), pp. 2946–2959

[2] Liu, G., Chen, B., Wang, K., Song, X.: 'Selective Current Harmonic Suppression for High-Speed PMSM Based on High-Precision Harmonic Detection Method', IEEE Transactions on Industrial Informatics, 2018, pp. 1–1

[3] Doppelbauer, M., Winzer, P.: 'A lighter motor for tomorrow's electric car', IEEE Spectrum, 2017, 54, (7), pp. 26–31

[4] Adamczyk, D., Wilk, A., Michna, M.: 'Model of the double-rotor induction motor in terms of electromagnetic differential', Archives of Electrical Engineering, 2016, 65, (4), pp. 761–772

[5] Gerada, D., Zhang, H., Xu, Z., Calzo, G.L., Gerada, C.: 'Electrical Machine Type Selection for High Speed Supercharger Automotive Applications'. Proc. 19th International Conference on Electrical Machines and Systems (ICEMS), 2016, pp. 1–6

[6] Zabaleta, M., Jones, M., Levi, E.: 'A tuning procedure for the current regulator loops in multiple three-phase permanent magnet machines with low switching to fundamental frequency ratio', Proc. 19th European Conference on Power Electronics and Applications (EPE'17 ECCE Europe), 2017, pp. 1–10

[7] Sahoo, S.K., Bhattacharya, T.: 'Rotor Flux-Oriented Control of Induction Motor With Synchronized Sinusoidal PWM for Traction Application', IEEE Transactions on Power Electronics, 2016, 31, (6), pp. 4429–4439

[8] Kwon, Y.-C., Kim, S., Sul, S.-K.: 'Six-Step Operation of PMSM With Instantaneous Current Control', IEEE Transactions on Industry Applications, 2014, 50, (4), pp. 2614–2625

[9] Sepulchre, L., Fadel, M., Pietrzak-David, M.: 'Improvement of the digital control of a high speed PMSM for vehicle application'. Proc. Eleventh International Conference on Ecological Vehicles and Renewable Energies (EVER), 2016, pp. 1–9

[10] Jarzebowicz, L.: 'Modeling the impact of discretizing rotor angular position on computation of field-oriented current components in high speed electric drives', Applied Mathematical Modelling, 2017, 42, pp. 576–590

[11] Oleschuk, V., Barrero, F.: 'Standard and Non-Standard Approaches for Voltage Synchronization of Drive Inverters with Space-Vector PWM: a Survey', International Review of Electrical Engineering (IREE), 2014, 9, (4), pp. 688–707

[12] Tarczewski, T., Grzesiak, L.M.: 'Constrained State Feedback Speed Control of PMSM Based on Model Predictive Approach', IEEE Transactions on Industrial Electronics, 2016, 63, (6), pp. 3867–3875

[13] Sandre-Hernandez, O., Rangel-Magdaleno, J., Morales-Caporal, R.: 'A Comparison on Finite-Set Model Predictive Torque Control Schemes for PMSMs', IEEE Transactions on Power Electronics, 2018, 33, (10), pp. 8838–8847

[14] Ahmed, A.A., Koh, B.K., Lee, Y.I.: 'A Comparison of Finite Control Set and Continuous Control Set Model Predictive Control Schemes for Speed Control of Induction Motors', IEEE Transactions on Industrial Informatics, 2018, 14, (4), pp. 1334–1346

[15] Belda, K., Vosmik, D.: 'Explicit Generalized Predictive Control of Speed and Position of PMSM Drives, 'IEEE Transactions on Industrial Electronics, 2016, 63, (6), pp. 3889–3896

[16] Siami, M., Khaburi, D.A., Rodríguez, J.: 'Torque Ripple Reduction of Predictive Torque Control for PMSM Drives With Parameter Mismatch', IEEE Transactions on Power Electronics, 2017, 32, (9), pp. 7160–7168
[17] Jarzebowicz, L.: 'Impact of low switching-to-fundamental frequency ratio on predictive current control of PMSM: A simulation study'. Proc. 25th International Workshop on Electric Drives: Optimization in Control of Electric Drives (IWED), 2018, pp. 1–5
[18] Anuchin, A., Briz, F., Shpak, D., Lashkevich, M.: 'PWM strategy for 3-phase 2-level VSI with non-idealities compensation and switching losses minimization'. Proc. IEEE International Electric Machines and Drives Conference (IEMDC), 2017, pp. 1–6
[19] Persson, E.: 'Motor current measurement using time-modulated signals'. Proc. Power Conversion Conference PCC, Osaka 2002, pp. 716–720
[20] Wolf, C.M., Degner, M.W., Briz, F.: 'Analysis of Current Sampling Errors in PWM VSI Drives', IEEE Transactions on Industry Applications, 2015, 51, (2), pp. 1551–1560
[21] Jarzebowicz, L.: 'Errors of a Linear Current Approximation in High-Speed PMSM Drives', IEEE Transactions on Power Electronics, 2017, 32, (11), pp. 8254–8257
[22] Wang, H., Yang, M., Niu, L., Xu, D.: 'Current-loop bandwidth expansion strategy for permanent magnet synchronous motor drives'. Proc. 5th IEEE Conference on Industrial Electronics and Applications (ICIEA), 2010, pp. 1340–1345
[23] Zhang, Y., Huang, L., Xu, D., Liu, J., Jin, J.: 'Performance evaluation of two-vector-based model predictive current control of PMSM drives', Chinese Journal of Electrical Engineering, 2018, 4, (2), pp. 65–81
[24] Wang, W., Fan, Y., Chen, S., Zhang, Q.: 'Finite control set model predictive current control of a five-phase PMSM with virtual voltage vectors and adaptive control set', CES Transactions on Electrical Machines and Systems, 2018, 2, (1), pp. 136–141
[25] Jarzebowicz, L., Mirchevski, S.: 'Modeling the impact of rotor movement on non-linearity of motor currents waveforms in high-speed PMSM drives', Proc. 19th European Conference on Power Electronics and Applications EPE'2017 ECCE Europe, Warsaw, 2017.